ORGANOMETALLICS

Article

Cite This: *Organometallics* 2019, 38, 1468−1478

pubs.acs.org/Organometallics

Dehydrogenative Coupling of Aldehydes with Alcohols Catalyzed by a Nickel Hydride Complex

Nathan A. Eberhardt, Nadeesha P. N. Wellala, Yingze Li, Jeanette A. Krause, and Hairong Guan*

Department of Chemistry, University of Cincinnati, P.O. Box 210172, Cincinnati, Ohio 45221-0172, United States

Supporting Information

A nickel hydride complex, {2,6-(^{i}Pr$_2$PO)$_2$C$_6$H$_3$}NiH, has been shown to catalyze the coupling of RCHO and R′OH to yield RCO$_2$R′ and RCH$_2$OH, where the aldehyde also acts as a hydrogen acceptor and the alcohol also serves as the solvent. Functional groups tolerated by this catalytic system include CF$_3$, NO$_2$, Cl, Br, NHCOMe, and NMe$_2$, whereas phenol-containing compounds are not viable substrates or solvents. The dehydrogenative coupling reaction can alternatively be catalyzed by an air-stable nickel chloride complex, {2,6-(^{i}Pr$_2$PO)$_2$C$_6$H$_3$}NiCl, in conjunction with NaOMe. Acids in unpurified aldehydes react with the hydride to form nickel carboxylate complexes, which are catalytically inactive. Water, if present in a significant quantity, decreases the catalytic efficiency by forming {2,6-(^{i}Pr$_2$PO)$_2$C$_6$H$_3$}NiOH, which causes catalyst degradation. On the other hand, in the presence of a drying agent, {2,6-(^{i}Pr$_2$PO)$_2$C$_6$H$_3$}NiOH generated in situ from {2,6-(^{i}Pr$_2$PO)$_2$C$_6$H$_3$}NiCl and NaOH can be converted to an alkoxide species, becoming catalytically competent. The proposed catalytic mechanism features aldehyde insertion into the nickel hydride as well as into a nickel alkoxide intermediate, both of which have been experimentally observed. Several mechanistically relevant nickel species including {2,6-(^{i}Pr$_2$PO)$_2$C$_6$H$_3$}-NiOC(O)Ph, {2,6-(^{i}Pr$_2$PO)$_2$C$_6$H$_3$}NiOPh, and {2,6-(^{i}Pr$_2$PO)$_2$C$_6$H$_3$}NiOPh·HOPh have been independently synthesized, crystallographically characterized, and tested for the catalytic reaction. While phenol-containing molecules cannot be used as substrates or solvents, both {2,6-(^{i}Pr$_2$PO)$_2$C$_6$H$_3$}NiOPh and {2,6-(^{i}Pr$_2$PO)$_2$C$_6$H$_3$}NiOPh·HOPh are efficient in catalyzing the dehydrogenative coupling of PhCHO with EtOH.

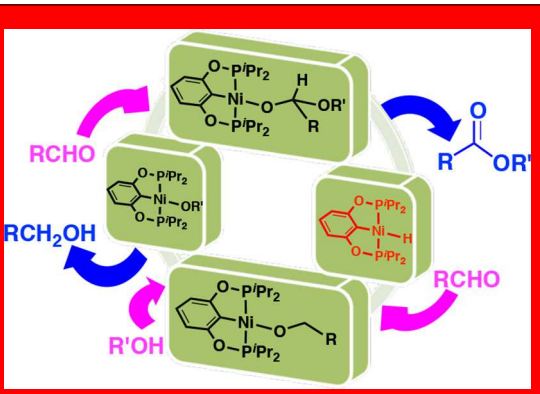

INTRODUCTION

Catalytic disproportionation of aldehydes to esters, also known as the Tishchenko reaction, provides a straightforward route to esters with the general formula RCO$_2$CH$_2$R (Scheme 1A).[1] An alternative synthetic method involves catalytic coupling of two molecules of RCH$_2$OH with the concomitant loss of four hydrogen atoms (Scheme 1B), either in the form of H$_2$ (i.e., acceptorless dehydrogenation)[2,3] or assisted by a hydrogen acceptor[4] or an oxidant.[5] Making esters of the type RCO$_2$R′ (R′ ≠ CH$_2$R) would require two different aldehydes[6] or alcohols[7] to construct the ester C−O bond. In these cases, selectivity for cross-coupling over homocoupling products is generally poor, unless one substrate is added in large excess or two electronically biased ones are employed.[8] Beyond the traditional esterification strategies focused on the reaction between RCO$_2$H and R′OH, catalytic dehydrogenative coupling of aldehydes with alcohols has been developed as a greener method to synthesize esters with diverse structures.[9] As inferred by the balanced equation (Scheme 1C), to form one RCO$_2$R′ molecule, two hydrogen atoms must be removed. This can be accomplished in an acceptorless fashion,[10] by using a sacrificial hydrogen acceptor[11] or an oxidant,[12] or under electrochemical conditions.[13]

On what appeared to be a completely different research path, we studied {2,6-(^{i}Pr$_2$PO)$_2$C$_6$H$_3$}NiH (**1**) as a catalyst for the hydrosilylation of aldehydes with PhSiH$_3$[14] as well as the reduction of CO$_2$ with HBcat (HBcat = catecholborane) to yield CH$_3$OBcat and catBOBcat.[15] The latter reaction was shown to proceed via hydroboration of HCHO as the last stage of the catalytic process. In attempts to replace the silane and

Scheme 1. Synthesis of Esters from Aldehydes and/or Alcohols

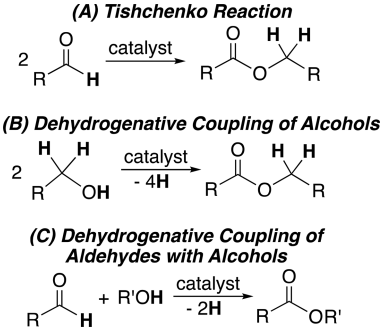

Received: December 8, 2018
Published: March 13, 2019

DOI: 10.1021/acs.organomet.8b00888
Organometallics 2019, 38, 1468−1478

the borane with H_2 as a cheaper source of reductant, we explored the possibility of utilizing **1** to catalyze the hydrogenation of benzaldehyde (Scheme 2). The reaction

Scheme 2. Attempted Hydrogenation of Benzaldehyde in Different Solvents

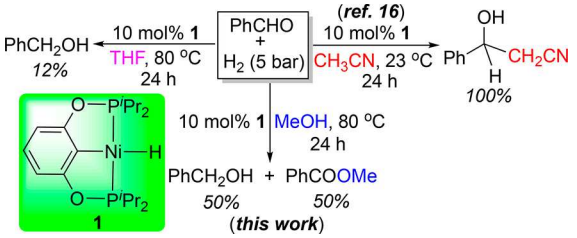

carried out in THF produced a small amount of $PhCH_2OH$, likely due to stoichiometric reduction of PhCHO by the nickel hydride.[14] In contrast, using CH_3CN as the solvent resulted in catalytic cyanomethylation of PhCHO, a process that does not need H_2.[16] A significant amount of $PhCH_2OH$ was, however, obtained when the solvent was switched to MeOH. The failure to observe any H_2 uptake hinted to us that the reaction was not a hydrogenation process either. After a closer inspection, $PhCO_2Me$ was identified as the second product in similar quantity to $PhCH_2OH$, implying that PhCHO itself acted as a hydrogen acceptor for the dehydrogenative coupling of PhCHO with MeOH.

To our knowledge, there is only one previous example of homogeneous nickel-catalyzed dehydrogenative coupling of aldehydes with alcohols, which uses an *N*-heterocyclic carbene (NHC) ligated Ni(0) species as the catalyst and $PhCOCF_3$ as the hydrogen acceptor.[11b] The proposed mechanism involves oxidative addition of the aldehyde C−H bond to nickel. Such a step is highly unlikely to occur with our Ni(II) hydride, suggesting that our reaction operates by a different mechanism. Given that nickel-catalyzed dehydrogenative coupling reactions in general are rare in the literature,[11b,17] we decided to investigate our catalytic system in greater detail, particularly concerning the mechanism. The obtained mechanistic information not only helps improve the dehydrogenative coupling reaction but also uncovers many pitfalls associated with the reactions of metal hydrides with aldehydes. With these goals in mind, we examined the substrate scope for the esterification of RCHO with R′OH catalyzed by **1**, characterized several nickel species relevant to the catalytic cycles, and investigated the roles that impurities could play during the dehydrogenative coupling process.

RESULTS AND DISCUSSION

Reaction Optimization and Substrate Scope. The nickel-catalyzed dehydrogenative coupling of PhCHO with MeOH was further investigated by varying the temperature and catalyst loading. A similar transformation of PhCHO and EtOH to $PhCH_2OH$ and $PhCO_2Et$ was also examined in this context. As shown in Table 1, the esterification reaction can take place at room temperature although the rate is greatly accelerated by mild heating (80 °C). The catalyst loading (with respect to the total PhCHO) can be lowered to 1 mol % (entries 5 and 6) or even 0.1 mol % under neat conditions (entry 7), resulting in a turnover number of 456 for producing $PhCO_2Me$. In each experiment, the Tishchenko product $PhCO_2CH_2Ph$ is either negligible or below the NMR detection

Table 1. Catalytic Dehydrogenative Coupling of Benzaldehyde with Methanol or Ethanol[a]

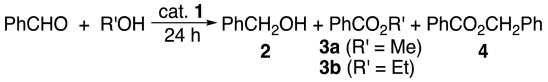

entry	**1** (mol %)	R′OH	temperature (°C)	conversion of PhCHO (%)[c]	**2**:**3a**/**3b**:**4**[c]
1	10	MeOH	80	100	50:50:0
2	10	EtOH	80	100	50:50:0
3	10	MeOH	23	65	54:46:0
4	10	EtOH	23	20	75:25:0
5	1	MeOH	80	100	50:50:trace
6	1	EtOH	80	99	50:50:0
7[b]	0.1	MeOH	80	93	49:49:2
8[b]	0.1	MeOH	60	8	50:50:0

[a]Standard conditions: a mixture of PhCHO (0.20 or 2.0 mmol) and **1** (0.020 mmol) in 1.0 mL of R′OH stirred for 24 h. [b]A mixture of PhCHO (20 mmol), MeOH (10 mmol), and **1** (0.020 mmol) stirred for 24 h. [c]Determined by ^{1}H NMR spectroscopy using mesitylene as the internal standard.

limit. The amount of $PhCH_2OH$ generated is equal to the amount of $PhCO_2R'$ when the reaction goes to completion or the catalyst loading is ≤1 mol %. However, at a high catalyst loading, when the conversion of PhCHO is low (entries 3 and 4), there is an excess of $PhCH_2OH$ found in the product mixture. The presence of surplus $PhCH_2OH$ is an indication that PhCHO reduction occurs before ester formation.

In the aforementioned reaction, MeOH or EtOH acts as both substrate and solvent. Attempts were made to determine if a nonalcoholic solvent could be used for the dehydrogenative coupling process (Table 2). Unfortunately, changing the

Table 2. Catalytic Dehydrogenative Coupling of Benzaldehyde with Ethanol in Different Solvents[a]

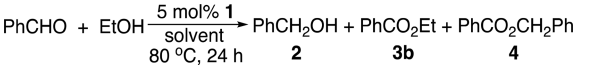

entry	solvent	conversion of PhCHO (%)[c]	**2**:**3b**:**4**[c]
1[b]	EtOH	100	50:50:0
2	THF	44	56:42:2
3	toluene	10	74:26:0
4	DMSO	8	91:6:3
5	DMF	24	61:36:3
6	glyme	17	53:47:0
7	diglyme	10	92:8:0

[a]Standard conditions: a mixture of PhCHO (0.40 mmol), EtOH (2.0 mmol), and **1** (0.020 mmol) in 1.0 mL of solvent stirred at 80 °C for 24 h. [b]A mixture of PhCHO (0.40 mmol) and **1** (0.020 mmol) in 1.0 mL of EtOH stirred at 80 °C for 24 h. [c]Determined by ^{1}H NMR spectroscopy using mesitylene as the internal standard.

solvent to THF or toluene resulted in a low conversion of PhCHO. To ensure that the diminished reactivity was not due to a decrease in solvent polarity, polar solvents such as DMSO, DMF, glyme, and diglyme were tested. These solvents all turned out to be inferior media for carrying out the catalytic dehydrogenative coupling of PhCHO with EtOH.

The scope of alcohols for the dehydrogenative reaction (performed in the alcohol of interest) was explored using benzaldehyde as the coupling partner with a catalyst loading of 5 mol %. As shown in Table 3, methanol and ethanol proceed

DOI: 10.1021/acs.organomet.8b00888
Organometallics 2019, 38, 1468−1478

Table 3. Catalytic Dehydrogenative Coupling of Benzaldehyde with Different Alcohols[a]

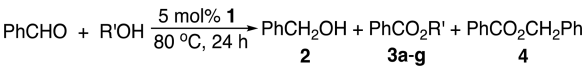

entry	R′OH	$PhCO_2R'$	conversion of PhCHO (%)[d]	2:3a–3g:4[d]
1	MeOH	**3a**	100	50:50:0
2	EtOH	**3b**	100	50:50:0
3	^{n}PrOH	**3c**	72	53:47:0
4[b]	^{i}PrOH	**3d**	98	57:39:1
5[c]	PhCH(OH)Me	**3e**	84	81:19:0
6	^{t}BuOH	**3f**	5	100:0:0
7	PhOH	**3g**	0	

[a]Standard conditions: a mixture of PhCHO (0.40 mmol) and **1** (0.020 mmol) in 1.0 mL of R′OH stirred at 80 °C for 24 h. [b]Acetone observed from the product mixture. [c]Acetophenone observed from the product mixture. [d]Determined by ^{1}H NMR spectroscopy using mesitylene as the internal standard.

well, affording $PhCH_2OH$ and $PhCO_2R'$ in a 50:50 ratio. With *n*-propanol, the catalytic efficiency drops substantially (entry 3), suggesting that the reaction is most effective with short-chain alcohols. The use of secondary alcohols is complicated by the competing transfer hydrogenation of PhCHO, resulting in a higher $PhCH_2OH$-to-$PhCO_2R'$ ratio and the formation of a ketone byproduct (entries 4 and 5). A more bulky alcohol, ^{t}BuOH, shuts down the catalytic process completely, providing $PhCH_2OH$ in 5% yield as a result of stoichiometric reduction of PhCHO (entry 6). The reaction carried out in phenol does not even produce $PhCH_2OH$, implying that phenol is incompatible with the nickel hydride.

Functional group tolerance was probed by introducing various substituents such as CF_3, NO_2, Cl, Br, NHCOMe, NMe_2, and OH to the *para* position of benzaldehyde (Table 4). Under the typical catalytic conditions (5 mol % catalyst loading, 80 °C, 24 h), most of these substituted benzaldehydes reacted smoothly with methanol to give an equimolar mixture of $ArCH_2OH$ and $ArCO_2Me$ with a combined yield of 95–99% (entries 1–5). In contrast, the reaction of 4-(dimethylamino)benzaldehyde was sluggish, only achieving a total yield of 41% for the alcohol and the methyl ester (entry 6). 4-Hydroxybenzaldehyde was shown to be a problematic substrate for the catalytic reaction (entry 7), once again demonstrating the incompatibility of the phenol group with the nickel hydride. To understand the substituent effects on the reaction rates, the catalytic reaction was stopped after 1 h instead of 24 h. It became evident that aldehydes bearing an electron-withdrawing group (e.g., CF_3, NO_2, Cl, or Br) reacted faster than those containing an electron-donating group (e.g., NHCOMe or NMe_2).

Table 4. Catalytic Dehydrogenative Coupling of Different Aldehydes with Methanol[a]

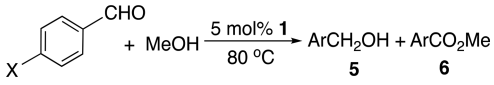

entry	X	yield after 24 h (%)[b,c]	5:6 (after 24 h)[c]	conversion after 1 h (%)[c]	5:6 (after 1 h)[c]
1	CF_3	99	50:50	93	50:50
2	NO_2	96	52:48	57	55:45
3	Cl	98	50:50	40	58:42
4	Br	95	51:49	58	56:44
5	NHCOMe	97	50:50	22	56:44
6	NMe_2	41	52:48	9	70:30
7	OH	5	100:0	0	0:0

[a]Standard conditions: a mixture of ArCHO (0.40 mmol) and **1** (0.020 mmol) in 1.0 mL of MeOH stirred at 80 °C. [b]Combined NMR yield of **5** and **6**. [c]Determined by ^{1}H NMR spectroscopy using mesitylene as the internal standard.

Mechanistic Studies. One limitation of our catalytic system lies in the fact that 50% of the aldehydes are sacrificed as hydrogen acceptors. To overcome this shortcoming, a deeper understanding of the reaction mechanism is needed. For dehydrogenative coupling of aldehydes with alcohols catalyzed by $Ni(COD)_2$/IPr (COD = 1,5-cyclooctadiene, IPr = 1,3-bis(2,6-diisopropylphenyl)imidazol-2-ylidene),[11b] Whittaker and Dong have proposed an acyl nickel hydride intermediate resulting from oxidative addition of the aldehyde C_{sp2}–H bond (Scheme 3). The subsequent carbonyl insertion of $PhCOCF_3$ provides an acyl nickel alkoxide species, which undergoes alkoxide exchange with the alcohol to be coupled. The catalytic cycle is closed by a reductive elimination step to release the ester product.

Scheme 3. Mechanism Proposed for Ni(0)-NHC-Catalyzed Dehydrogenative Coupling of Aldehydes with Alcohols[11b]

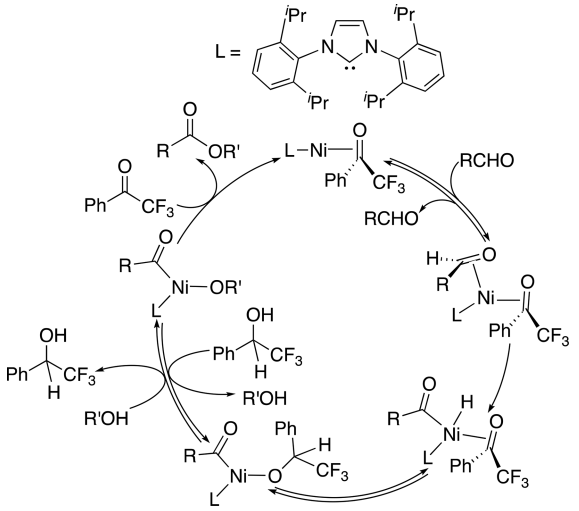

Our system employs a well-defined nickel hydride complex directly as the catalyst. Carbonyl insertion into the Ni–H bond, as postulated above, can be readily observed here by NMR spectroscopy. In C_6D_6, the insertion rate correlates well with the electrophilicity of the carbonyl group (i.e., 4-$CF_3C_6H_4CHO$ > C_6H_5CHO > 4-$Me_2NC_6H_4CHO$). ^{2}H NMR studies of the reaction of the nickel deuteride (**1-d_1**) with 2 equiv of 4-XC_6H_4CHO (in C_6H_6) suggest that the insertion is irreversible at room temperature but reversible at 50 °C (Scheme 4). Of the three substrates examined, the insertion product originating from **1-d_1** and 4-$CF_3C_6H_4CHO$ undergoes H/D exchange with the surplus aldehyde to the least extent (~5% over 24 h). This is not due to an equilibrium isotope effect but rather to a kinetic phenomenon.[18] A stronger Ni–O bond rendered by the electron-withdrawing CF_3 group[19] may provide a ground-state stabilization that disfavors the *β*-hydride elimination. Attempts to isolate the insertion products in a pure form failed, in part due to their high

DOI: 10.1021/acs.organomet.8b00888
Organometallics 2019, 38, 1468–1478

Scheme 4. Reversibility of Aldehyde Insertion Probed by Deuterium-Labeling Experiments

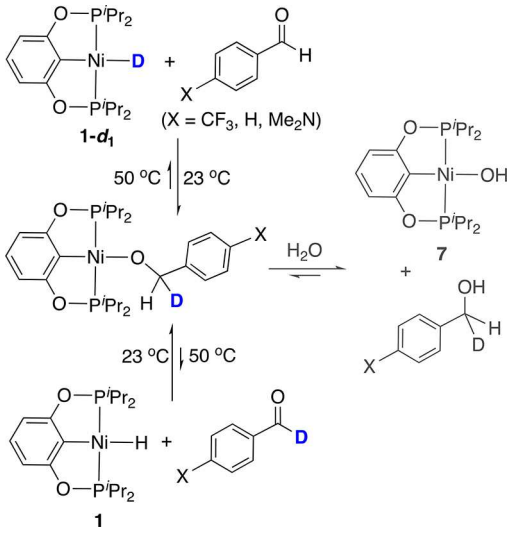

sensitivity toward adventitious water.[14] In fact, treatment of the insertion products with water was shown to yield free alcohols along with {2,6-(^{i}Pr$_2$PO)$_2$C$_6$H$_3$}NiOH (**7**), which also decomposed rapidly during workup.[20,21]

The reaction of **1** with ~3 equiv of 4-$CF_3C_6H_4CHO$ in C_6D_6 offered more mechanistic insights. In addition to the expected insertion product **8** (Scheme 5) along with a trace amount of **7** due to hydrolysis, another nickel pincer complex **9** was detected as a minor product (~30%). Its ^{1}H NMR spectrum features an AB quartet at 4.47 and 4.31 ppm (J_{AB} = 12.8 Hz) and a singlet at 5.65 ppm (integrated to a 2:1 ratio), consistent with a nickel species formed by two consecutive insertions of the aldehyde. Heating the solution to 80 °C resulted in a gradual disappearance of **9** and the aldehyde with concomitant appearance of ester **10**, presumably through a β-hydride elimination process. The steps illustrated in Scheme 5 essentially complete a catalytic cycle for generating the Tishchenko product. After 24 h of heating, the reaction mixture consisted of **8** (44%), **9** (0.5%), **10** (46%), 4-$CF_3C_6H_4CH_2OH$ (6%), 4-$CF_3C_6H_4CHO$ (1.5%), and other unidentified species (2%). The nickel hydride was absent from this mixture, suggesting that the first insertion event is the fastest step within the cycle. On the basis of our previous observation of a facile deinsertion of PhCHO from {2,6-(^{i}Pr$_2$PO)$_2$C$_6$H$_3$}NiOCH(CH$_2$CN)Ph (eq 1),[16] we propose

Scheme 5. Ester Formation via Consecutive Insertions of an Aldehyde

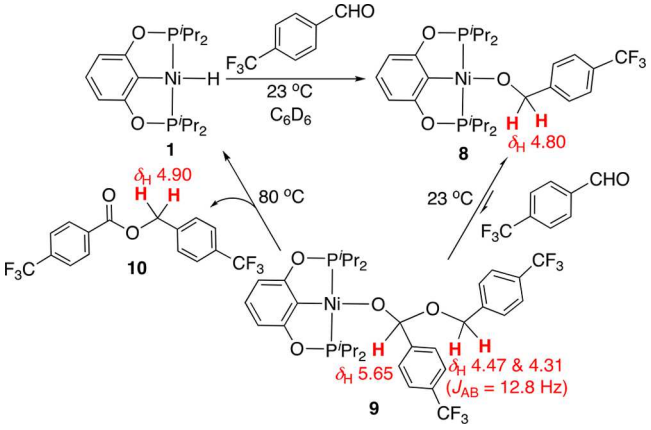

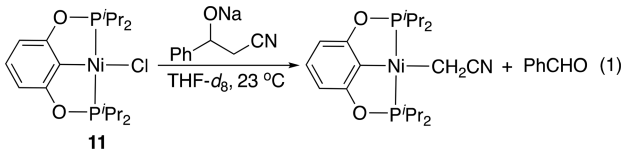

that the second insertion step converting **8** to **9** is reversible. Although increasing the temperature would reduce the steady-state concentration of **9** (due to entropic effect), it allows the elimination of **10** to occur more rapidly.

In an alcoholic solvent, R′OH, the alcohol is likely to intercept the insertion products like **8** to yield {2,6-(^{i}Pr$_2$PO)$_2$C$_6$H$_3$}NiOR′, which in turn reacts with aldehydes in a similar fashion as **8** (i.e., aldehyde insertion followed by β-hydride elimination). It should be noted that **1** dissolved in CD_3OD was slowly converted to {2,6-(^{i}Pr$_2$PO)$_2$C$_6$H$_3$}-$NiOCD_3$ (**12-d_3**) and HD (triplet at 4.52 ppm, $J_{H\text{-}D}$ = 42.8 Hz) with a 71% conversion achieved in 48 h.[22] However, this process is much less competitive than aldehyde insertion into **1**. For instance, mixing **1** with 10 equiv of PhCHO in CD_3OD provided **12-d_3** and $PhCH_2OD$ almost instantaneously without forming HD. The ester product $PhCO_2CD_3$ grew over time, accompanied by an increase in the amount of $PhCH_2OD$. The reaction became more favorable when the temperature was raised to 80 °C (see Supporting Information for details).

The protonation of **1** with CD_3OD described above and the reversibility of aldehyde insertion demonstrated in Scheme 4 imply that the nickel hydride may catalyze dehydrogenative coupling of primary alcohols to esters (i.e., the reaction in Scheme 1B). Unfortunately, heating a mixture of **1** (1 mol % catalyst loading) and $PhCH_2OH$ at 80 °C for 24 h yielded only a trace amount of $PhCO_2CH_2Ph$. Although β-hydride elimination from {2,6-(^{i}Pr$_2$PO)$_2$C$_6$H$_3$}NiOCH$_2$Ph is kinetically accessible, it is thermodynamically too uphill to produce enough PhCHO.

A mechanism consistent with our experimental data is outlined in Scheme 6. Both the dehydrogenative coupling cycle and the Tishchenko cycle start with aldehyde insertion into the nickel hydride and finish with β-hydride elimination following aldehyde insertion into a nickel alkoxide species. The difference arises from which alkoxide species participates in the second insertion step. Thus, the equilibrium for the alkoxide exchange on nickel and the relative reactivity of nickel alkoxide species toward aldehydes determine the selectivity. For the reaction performed in R′OH, the equilibrium is shifted far to the {2,6-(^{i}Pr$_2$PO)$_2$C$_6$H$_3$}NiOR′ side, which initiates the dehydrogenative coupling process unless its reaction with aldehydes is unfavorable.

Our proposed mechanism differs significantly from that of Whittaker and Dong (Scheme 3),[11b] particularly regarding the change (or the lack thereof) in nickel oxidation state. Although we cannot rigorously rule out the possibility of forming a Ni(0) species via C_{ipso}–H reductive elimination from **1**,[22] the facile aldehyde insertion observed with the hydride makes us prefer the Ni(II)-only pathway (Scheme 6). Our mechanism is more analogous to the one proposed by Liu and Eisen for the dehydrogenative coupling of aldehydes with alcohols catalyzed by actinide alkoxides (in the presence of $PhCOCF_3$ as a hydrogen acceptor).[11c] The actinide system, however, invokes

DOI: 10.1021/acs.organomet.8b00888
Organometallics 2019, 38, 1468–1478

Scheme 6. Catalytic Cycles Proposed for Ester Formation Catalyzed by the Pincer Nickel Hydride Complex

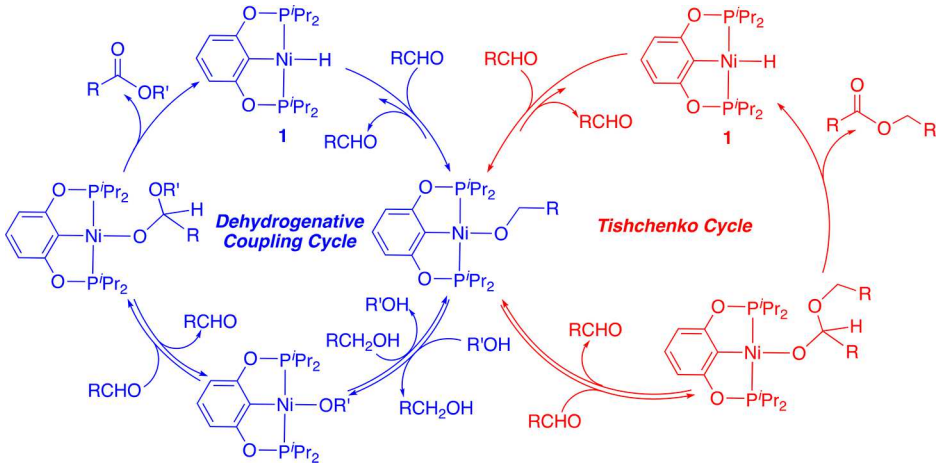

a Meerwein−Ponndorf−Verley type reduction of the hydrogen acceptor instead of the reduction by a metal hydride.

An alternative mechanism may involve a nickel-catalyzed Tishchenko reaction followed by a transesterification process. To discern this mechanistic scenario, a reaction profile for catalytic dehydrogenative coupling of PhCHO with EtOH was examined. As illustrated in Figure 1, the major pathway appears

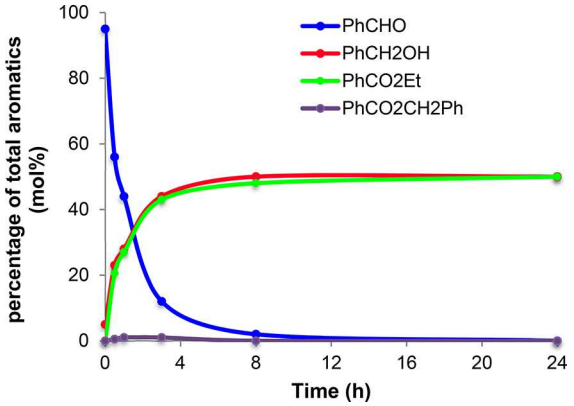

Figure 1. Reaction profile for nickel-catalyzed dehydrogenative coupling of PhCHO and EtOH (conditions: 0.40 mmol of PhCHO and 0.020 mmol of **1** in 1.0 mL of EtOH stirred at 80 °C).

to be the direct formation of $PhCO_2Et$, as evidenced by a very small amount of $PhCO_2CH_2Ph$ observed throughout the catalytic reaction. A possibility is that the transesterification process was too fast to allow a substantial accumulation of the Tishchenko product. However, a control experiment confirmed that the nickel hydride hardly catalyzed the transesterification of $PhCO_2CH_2Ph$ in EtOH (eq 2). These results

$$PhCO_2CH_2Ph + EtOH \xrightarrow[80\ ^oC,\ 24\ h]{5\ mol\%\ \mathbf{1}} PhCO_2Et + PhCH_2OH \quad (2)$$
(solvent)
3% conversion

indicate that while it is not impossible to form the Tishchenko product first and then the transesterification product, such a route is not a major pathway leading to $PhCO_2Et$.

Using a Nickel Chloride Complex as a Precatalyst. Because POCOP-pincer ligated nickel alkoxide complexes can form in situ by mixing the corresponding nickel chloride complexes with sodium or potassium alkoxides,[20a,23] we were curious to see if {2,6-(^{i}Pr$_2$PO)$_2$C$_6$H$_3$}NiCl (**11**) could serve as a precatalyst. Such an experiment would indirectly support our proposed mechanism (Scheme 6). Indeed, **11** in conjunction with NaOMe (in a 1:1 ratio) proved to be efficient and selective in converting PhCHO and EtOH to $PhCH_2OH$ and $PhCO_2Et$ (Table 5, entry 1). When NaOMe was replaced with

Table 5. Dehydrogenative Coupling of Benzaldehyde with Ethanol Using a Precatalyst[a]

$$PhCHO + EtOH \xrightarrow[80\ ^oC,\ 24\ h]{1\ mol\%\ \mathbf{11},\ 1\ mol\%\ base} \underset{\mathbf{2}}{PhCH_2OH} + \underset{\mathbf{3b}}{PhCO_2Et} + \underset{\mathbf{4}}{PhCO_2CH_2Ph}$$

entry	base	drying agent[b]	conversion of PhCHO (%)[c]	2:3b:4[c]
1	NaOMe		99	49:49:2
2	NaOH		8	0:0:100
3	NaOH	Na_2SO_4	92	48:46:6
4	NaOH	4 Å molecular sieves	95	49:49:2

[a]Standard conditions: a mixture of PhCHO (10 mmol), **11** (0.10 mmol), base (0.10 mmol), and EtOH (1.0 mL, 17 mmol) stirred at 80 °C for 24 h. [b]About 1 g of drying agent added. [c]Determined by ^{1}H NMR spectroscopy using mesitylene as the internal standard.

NaOH, the catalytic reaction became inefficient with only 8% of PhCHO converted, and the selectivity favored the Tishchenko product (entry 2). However, adding a drying agent such as anhydrous Na_2SO_4 or 4 Å molecular sieves drastically improved the reaction, resulting in up to 95% conversion of PhCHO primarily to $PhCH_2OH$ and $PhCO_2Et$.

The effects of base and drying agent can be rationalized by considering a hydroxide/ethoxide exchange equilibrium, highlighted in Scheme 7. For a closely related system involving a bis(phosphine)-based pincer ligand, Cámpora and co-workers have reported an equilibrium constant of $1.4(2) \times 10^{-3}$ favoring {2,6-(^{i}Pr$_2$PCH$_2$)$_2$C$_6$H$_3$}NiOH and EtOH.[24] Thus, combining **11** with NaOH, despite being carried out in EtOH, would yield **7** as the major nickel pincer species. This nickel hydroxide complex, generated in situ from {2,6-(^{i}Pr$_2$PO)$_2$C$_6$H$_3$}NiOTf and NaOH, was shown to react with PhCHO to yield $PhCO_2CH_2Ph$ and numerous intractable products. However, in the presence of a drying agent, the equilibrium is shifted to **13**, which enters into a productive cycle to generate $PhCH_2OH$ and $PhCO_2Et$ catalytically.

DOI: 10.1021/acs.organomet.8b00888
Organometallics 2019, 38, 1468−1478

Scheme 7. Proposed Activation of the Precatalyst and the Subsequent Reactions

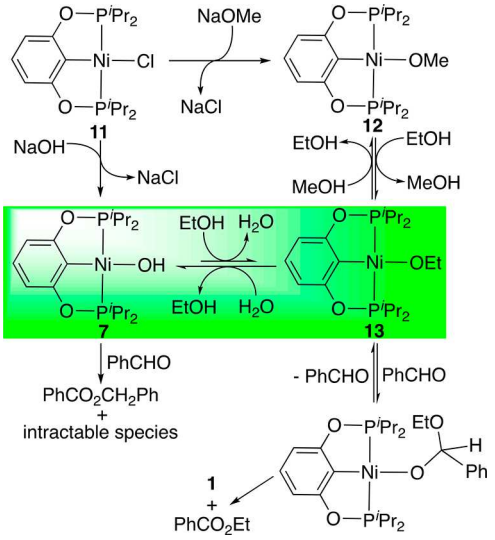

Deactivation of the Catalyst. Throughout our study, a number of species including impurities present in aldehydes, water, and phenols were shown to retard or negatively impact the catalytic reaction. Aldehydes used in this work must be distilled or recrystallized prior to use. The main impurities in unpurified aldehydes are carboxylic acids originating from oxidation of the aldehydes. These acids may protonate the nickel hydride or nickel alkoxide intermediates, resulting in nickel carboxylate complexes that could be catalytically inactive. Water, though not necessarily intolerable, can be detrimental to the catalytic process, especially when it is present in a sufficient amount to shift the hydroxide/alkoxide exchange equilibrium to **7** (Scheme 7). Phenols may also be acidic enough to protonate the hydride to form catalytically inactive phenoxide species.

To further understand the roles that impurities can play and the reason why phenol is an incompatible functional group, independent syntheses of the postulated catalyst deactivation products were pursued. When **1** was mixed with $PhCO_2H$ in C_6D_6, the desired nickel carboxylate complex {2,6-(^{i}Pr$_2$PO)$_2$C$_6$H$_3$}NiOC(O)Ph (**14**) formed along with some decomposition products. Attempts to separate **14** from these byproducts were fruitless, so attention was turned to alternative routes. Analytically pure **14** was eventually obtained in high yield (92%) from a salt metathesis reaction between **11** and $PhCO_2Ag$, following a similar procedure developed for a nickel acetate complex.[25] The crystal structure of **14** (Figure 2) shows a κ^1-benzoate, which is perpendicular to the coordination plane. In contrast, our previously reported formate complex {2,6-(^{i}Pr$_2$PO)$_2$C$_6$H$_3$}NiOC(O)H adopts an in-plane conformation for the κ^1-formate.[15b] Otherwise, the bond metrics for the two complexes are almost identical. A control experiment using **14** as a catalyst (1 mol % loading) under the typical conditions (80 °C, 24 h, in EtOH) showed no conversion of PhCHO, confirming that protonation of **1** by acid impurities shuts down the catalytic reaction.

The observed hydrolysis of the insertion products to yield **7** (Scheme 4) and the unwanted reactions of **7** with PhCHO (Scheme 7) imply that water is harmful to the catalytic reaction. Alcohols used in this study were dried over CaH_2, distilled, and then further dried using 4 Å molecular sieves.

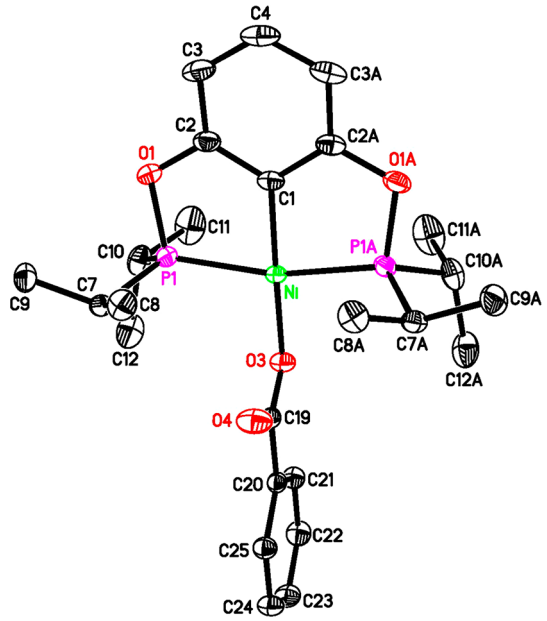

Figure 2. ORTEP drawing of {2,6-(^{i}Pr$_2$PO)$_2$C$_6$H$_3$}NiOC(O)Ph (**14**) at the 50% probability level (hydrogen atoms omitted for clarity). Selected bond lengths (Å) and angles (deg): Ni−C(1) 1.8818(15), Ni−O(3) 1.9096(11), Ni−P(1) 2.1609(3), Ni−P(1A) 2.1609(3), C(19)−O(3) 1.2853(18), C(19A)−O(4) 1.2341(18); C(1)−Ni(1)−O(3) 175.83(5), P(1)−Ni−P(1A) 163.574(17).

When water (100 equiv with respect to PhCHO) was added intentionally to the reaction mixture, the conversion of PhCHO dropped to only 11% with some Tishchenko product being observed (eq 3).

$$\mathrm{PhCHO} + \mathrm{EtOH} \xrightarrow[80\ ^\circ\mathrm{C},\ 24\ \mathrm{h}]{1\ \mathrm{mol\%}\ \mathbf{1}} \underset{\mathbf{2}}{\mathrm{PhCH_2OH}} + \underset{\mathbf{3b}}{\mathrm{PhCO_2Et}} + \underset{\mathbf{4}}{\mathrm{PhCO_2CH_2Ph}} \quad (3)$$

without H_2O: 99% conv., **2** : **3b** : **4** = 50 : 50 : 0
with H_2O: 11% conv., **2** : **3b** : **4** = 50 : 48 : 2

Another catalyst deactivation pathway that has been implicated is specifically for reactions involving phenol-type molecules as either substrates or solvents. Considering the propensity of **1** and closely related nickel hydride complexes to undergo protonation by acids,[15a,26] we speculated that PhOH could protonate **1** to yield a nickel phenoxide complex along with dihydrogen. This was indeed observed from an NMR reaction carried out in C_6D_6 (eq 4). It was, however,

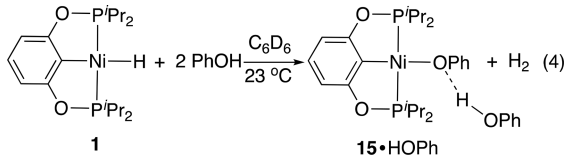

interesting to note that 2 equiv of PhOH was needed to fully protonate the hydride. An X-ray crystallographic study of the organometallic product revealed an adduct of {2,6-(^{i}Pr$_2$PO)$_2$C$_6$H$_3$}NiOPh (**15**) and PhOH bound by a hydrogen bond (Figure 3).

The nickel phenoxide complex free of phenol was obtained from the reaction of **11** with NaOPh (eq 5). Adding 1 equiv of PhOH to a solution of **15** in C_6D_6 reproduced the NMR spectra for the protonation reaction shown in eq 4. Apart from the lack of aromatic resonances attributed to the hydrogen

DOI: 10.1021/acs.organomet.8b00888
Organometallics 2019, 38, 1468−1478

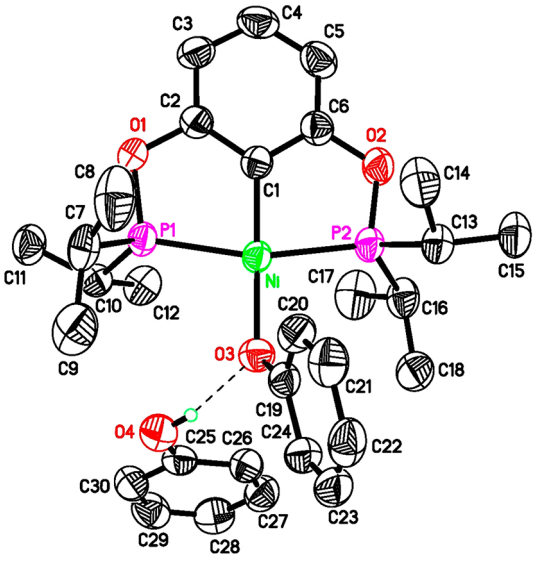

Figure 3. ORTEP drawing of {2,6-(^{i}Pr$_2$PO)$_2$C$_6$H$_3$}NiOPh·HOPh (**15**·HOPh) at the 50% probability level (all hydrogen atoms except the one involved in hydrogen bonding omitted for clarity). Selected bond lengths (Å) and angles (deg): Ni−C(1) 1.8834(18), Ni−O(3) 1.9147(13), Ni−P(1) 2.1907(6), Ni−P(2) 2.1890(6), C(19)−O(3) 1.342(2), C(25)−O(4) 1.359(3), O(4)−H 0.80(2), O(3)···H 1.87(2), O(3)···O(4) 2.664(2); C(1)−Ni−O(3) 179.67(7), P(1)−Ni−P(2) 163.02(2), O(4)−H···O(3) 168(3).

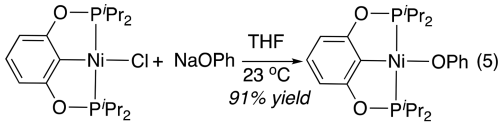

bonded PhOH, proton resonances of **15** are remarkably similar to those of **15**·HOPh. The ^{31}P resonance of **15** is shifted downfield by 0.35 ppm upon conversion to **15**·HOPh. As expected, in the absence of PhOH, the nickel center is less crowded (Figure 4). Consequently, going from **15**·HOPh to **15**, the Ni−P and Ni−O bonds are contracted by 0.02−0.03 and 0.02−0.04 Å, respectively. However, the Ni−C$_{ipso}$ bond distance remains unchanged at 1.88 Å and is almost identical to that in **14**. In our previous studies of POCOP-pincer ligated nickel thiolate,[19] isothiocyanate,[27] and azide complexes,[27] we have also shown that the Ni−C$_{ipso}$ bond distance is unaffected by its *trans* ligand.

Interestingly, the phenoxide complex **15** remains an active catalyst for the dehydrogenative coupling of PhCHO with EtOH, although it is less effective than the hydride complex **1** (eq 6). At 80 °C with a 1 mol % catalyst loading, 77% of

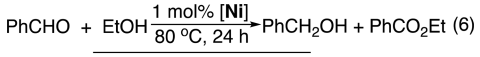

[Ni]	conv. of PhCHO
1	99%
15	77%
15•HOPh	95%

PhCHO was converted in 24 h, providing a 50:50 mixture of PhCH$_2$OH and PhCO$_2$Et with a negligible amount of PhCO$_2$CH$_2$Ph. This reaction catalyzed by **1** would have completed under the same conditions. Insertion of PhCHO into the Ni−OPh bond of **15** followed by the elimination of

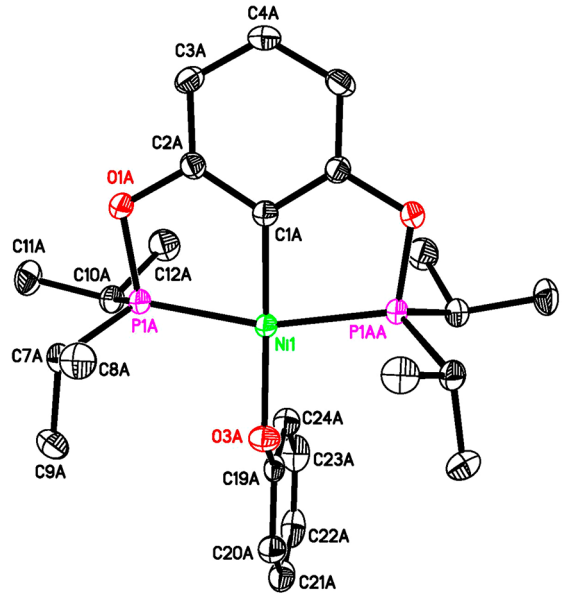

Figure 4. ORTEP drawing of {2,6-(^{i}Pr$_2$PO)$_2$C$_6$H$_3$}NiOPh (**15**) at the 50% probability level (hydrogen atoms omitted for clarity; only molecule A shown; only symmetry-unique carbon and oxygen atoms labeled). Selected bond lengths (Å) and angles (deg): Ni(1)−C(1A) 1.881(2), Ni(1)−O(3A) 1.8929(16), Ni(1)−P(1A) 2.1652(4), Ni(1)−P(1AA) 2.1653(4), C(19A)−O(3A) 1.322(3); C(1A)−Ni(1)−O(3A) 172.70(8), P(1A)−Ni(1)−P(1AA) 163.30(3).

PhCO$_2$Ph could generate the nickel hydride **1**. However, PhCO$_2$Ph was not observed (by GC-MS) throughout the catalytic reaction. Instead, free PhOH was detected, suggesting that **15** may undergo a phenoxide-ethoxide exchange with EtOH to yield the catalytically active {2,6-(^{i}Pr$_2$PO)$_2$C$_6$H$_3$}-NiOEt. Although a control experiment carried out in C$_6$D$_6$ showed no phenoxide-ethoxide exchange between **15** and EtOH (10 equiv), such a process might still be operative *in EtOH*. With an excess of PhOH, **1** should be converted to **15**·HOPh, and the hydrogen bonded PhOH presumably will block EtOH from approaching the nickel center for the phenoxide−ethoxide exchange. To our surprise, the in situ generated **15**·HOPh (by mixing **15** with 1 equiv of PhOH) was found to be catalytically more active than **15** but slightly less active than **1** (eq 6). At the moment, we do not fully understand the reasons behind the reactivity differences.

We propose that sterics (i.e., from the R′ group in {2,6-(^{i}Pr$_2$PO)$_2$C$_6$H$_3$}NiOR′) play a critical role in determining the insertion rate and ultimately the efficiency of the overall process. The fact that the catalytic reaction in MeOH is faster than that in EtOH, which is evident at room temperature (Table 1, entry 3 vs entry 4), can be explained by a more facile PhCHO insertion with {2,6-(^{i}Pr$_2$PO)$_2$C$_6$H$_3$}NiOMe (**12**). Based on the same argument, nickel *n*-propoxide and *t*-butoxide should be even less reactive than the ethoxide complex. Consistent with this hypothesis, the dehydrogenative coupling reaction is low yielding in ^{n}PrOH (Table 3, entry 3) while stopped in ^{t}BuOH (Table 3, entry 6). For secondary alcohols such as ^{i}PrOH and PhCH(OH)Me, because of the steric crowding, one would also expect a less efficient dehydrogenative coupling reaction. However, the conversion of PhCHO in these alcohols (Table 3, entries 4 and 5) is higher than the conversion in ^{n}PrOH. These results should not be interpreted as a sign of a fast PhCHO insertion. The

DOI: 10.1021/acs.organomet.8b00888
Organometallics 2019, 38, 1468−1478

observation of acetone and acetophenone as the byproducts suggests that the higher conversion of PhCHO is due to a competing transfer hydrogenation process.

CONCLUSIONS

In this work, we have carried out an in-depth study of dehydrogenative coupling of aldehydes with alcohols catalyzed by a nickel hydride complex. This catalytic system displays a moderate functional group tolerance and is compatible with various short-chain alcohols for the synthesis of esters. In doing so, one equivalent of aldehyde is consumed as a sacrificial hydrogen acceptor. Our mechanistic investigation supports a catalytic cycle composed of four steps: (1) aldehyde insertion into the nickel hydride, (2) alkoxide exchange between the resulting insertion product and the alcohol, (3) another aldehyde insertion step but with the nickel alkoxide intermediate, and (4) β-hydride elimination to release the ester product and regenerate the hydride. The competing Tishchenko reaction follows an analogous catalytic cycle, although it is suppressed due to the alkoxide exchange step mentioned above, which diverts the aldehyde to participate in the dehydrogenative coupling cycle. Guided by this mechanistic analysis, we have successfully replaced the air-sensitive nickel hydride catalyst with a nickel chloride complex as an air-stable precatalyst.

We have also examined potential catalyst deactivation pathways, which we believe have implications in other systems involving metal hydrides and aldehydes. In particular, we have shown that acid impurities in aldehydes can protonate the nickel hydride or the intermediates to form catalytically inactive nickel carboxylate complexes. Water, if present in a substantial amount, can decrease the catalytic efficiency by forming a nickel hydroxide complex leading to multiple decomposition pathways. Improvement of the catalytic system would require the development of new ligands that promote aldehyde insertion into the nickel alkoxide intermediate and, more importantly, bypass aldehyde insertion into the nickel hydride as well as alkoxide exchange for an acceptorless dehydrogenative coupling reaction. These are ongoing efforts in our laboratory.

EXPERIMENTAL SECTION

General Methods. All compounds described in this paper were prepared under an argon atmosphere using standard glovebox and Schlenk techniques. Benzene-d_6 was dried over Na-benzophenone and distilled under an argon atmosphere. Alcohols were dried over CaH_2, distilled under argon, and then stored with 4 Å molecular sieves. All other dry and oxygen-free solvents used for synthesis and workup (THF, toluene, and pentane) were collected from an Innovative Technology solvent purification system. Aldehydes were freshly distilled or recrystallized prior to use. {2,6-(^{i}Pr$_2$PO)$_2$C$_6$H$_3$}NiH (**1**),[14] {2,6-(^{i}Pr$_2$PO)$_2$C$_6$H$_3$}NiCl (**11**),[28] and {2,6-(^{i}Pr$_2$PO)$_2$C$_6$H$_3$}-NiOTf[28] were synthesized following literature procedures. {2,6-(^{i}Pr$_2$PO)$_2$C$_6$H$_3$}NiD (**1-d_1**) was prepared using the same procedure for making **1** except that $LiAlD_4$ was employed as the deuteride source. ^{1}H, ^{13}C{^{1}H}, and ^{31}P{^{1}H} NMR spectra were recorded on a Bruker Avance 400 MHz NMR spectrometer. ^{2}H NMR spectra were recorded on a Bruker Avance NEO 400 MHz NMR spectrometer. Chemical shift values in ^{1}H, ^{2}H, and ^{13}C{^{1}H} NMR spectra were referenced internally to the residual solvent resonances. ^{31}P{^{1}H} NMR spectra were referenced externally to 85% H_3PO_4 (0 ppm). Infrared spectra were recorded on a PerkinElmer Spectrum Two FT-IR spectrometer equipped with a smart orbit diamond attenuated total reflectance (ATR) accessory.

General Procedure for Catalytic Dehydrogenative Coupling of Aldehydes with Alcohols. To a flame-dried 5-dram scintillation vial equipped with a stir bar was added an aldehyde (2.0 mmol) and 1 mL of alcohol. Nickel hydride complex **1** (8.0 mg, 0.020 mmol, 1 mol % catalyst loading) was then added, and the vial was capped and wrapped with Parafilm to ensure appropriate sealing. The vial was placed in an 80 °C oil bath and heated at this temperature. After a given period of time, the vial was removed from the oil bath and cooled to room temperature in a water bath. Mesitylene (28 μL, 0.20 mmol) was then added as an internal standard. An aliquot of the reaction mixture was withdrawn and diluted with $CDCl_3$ for NMR analysis. Conversions of the aldehyde and product ratios were obtained from ^{1}H NMR integrations.

{2,6-(^{i}Pr$_2$PO)$_2$C$_6$H$_3$}NiOH (7) Generated in Situ. Under an argon atmosphere, freshly ground NaOH (12 mg, 0.30 mmol) was added to a solution of {2,6-(^{i}Pr$_2$PO)$_2$C$_6$H$_3$}NiOTf (50 mg, 0.091 mmol) in 0.5 mL of C_6D_6. The resulting orange suspension was vigorously stirred at room temperature for 30 min, during which time it turned to a gel-like material. C_6D_6 (1.0 mL) was added, and the mixture was then passed through a Titan3 PTFE syringe filter. The collected solution was analyzed by NMR spectroscopy. Attempts to isolate the product in a solid form through evaporation of the solvent led to significant decomposition. ^{1}H NMR (400 MHz, C_6D_6, δ): 6.85 (t, J_{H-H} = 8.0 Hz, Ar*H*, 1H), 6.56 (d, J_{H-H} = 8.0 Hz, Ar*H*, 2H), 2.17−2.07 (m, PC*H*(CH$_3$)$_2$, 4H), 1.41−1.34 (m, PCH(C*H*$_3$)$_2$, 12H), 1.28−1.22 (m, PCH(C*H*$_3$)$_2$, 12H), −2.45 (br, NiO*H*, 1H). ^{13}C{^{1}H} NMR (101 MHz, C_6D_6, δ): 169.50 (t, J_{P-C} = 10.4 Hz, ArC_{ortho}), 105.44 (t, J_{P-C} = 6.0 Hz, ArC_{meta}), 27.78 (t, J_{P-C} = 10.2 Hz, PCH(CH$_3$)$_2$), 17.25 (t, J_{P-C} = 3.6 Hz, PCH(*C*H$_3$)$_2$), 16.83 (s, PCH(*C*H$_3$)$_2$). ^{31}P{^{1}H} NMR (162 MHz, C_6D_6, δ): 178.49 (s).

Reaction of {2,6-(^{i}Pr$_2$PO)$_2$C$_6$H$_3$}NiOH (7) with PhCHO. To the in situ generated solution of **7** in C_6D_6 (as described above) was added 2.0 μL of PhCHO (20 μmol). The NMR spectra of the reaction mixture were recorded immediately. On the basis of integration of the aromatic resonances for **7** and the PhC*H*O resonance, the ratio between **7** and PhCHO was determined to be 1:0.9. The reaction was monitored at room temperature for 4 days by both ^{1}H and ^{31}P{^{1}H} NMR spectroscopy. The NMR spectra showed the formation of $PhCO_2CH_2Ph$ and at least 12 different phosphorus-containing products.

Monitoring the Catalytic Reaction by NMR Spectroscopy. Under an argon atmosphere, **1** (4.0 mg, 0.010 mmol) and PhCHO (10 μL, 0.10 mmol) were mixed with ∼0.4 mL of CD_3OD in a J. Young NMR tube. The reaction was monitored first at 23 °C and then at 80 °C by both ^{1}H and ^{31}P{^{1}H} NMR spectroscopy. At 23 °C, the reaction produced {2,6-(^{i}Pr$_2$PO)$_2$C$_6$H$_3$}NiOCD$_3$ (**12-d_3**) and $PhCH_2OD$ first, followed by a slow formation of $PhCO_2CD_3$ (13% in 16 h). At 80 °C, the reaction was complete within 24 h, producing a mixture of $PhCH_2OD$ and $PhCO_2CD_3$ along with **12-d_3** as the resting state of the catalyst. **12-d_3** was generated slowly (>48 h) by dissolving **1** in CD_3OD or rapidly by mixing {2,6-(^{i}Pr$_2$PO)$_2$C$_6$H$_3$}NiOTf with NaOMe in CD_3OD. ^{1}H NMR of **12-d_3** (400 MHz, CD_3OD, δ): 6.88 (t, J_{H-H} = 8.0 Hz, Ar*H*, 1H), 6.29 (d, J_{H-H} = 8.0 Hz, Ar*H*, 2H), 2.46−2.38 (m, PC*H*(CH$_3$)$_2$, 4H), 1.46−1.36 (m, PCH(C*H*$_3$)$_2$, 24H). ^{31}P{^{1}H} NMR of {2,6-(^{i}Pr$_2$PO)$_2$C$_6$H$_3$}NiOCD$_3$ (162 MHz, CD_3OD, δ): 176.90 (s).

Synthesis of {2,6-(^{i}Pr$_2$PO)$_2$C$_6$H$_3$}NiOC(O)Ph (14). Under an argon atmosphere, a suspension of **11** (100 mg, 0.23 mmol) and silver benzoate (62 mg, 0.27 mmol) in 25 mL of THF was stirred at room temperature in the absence of light for 6 h. The volatiles were removed under a vacuum, and the residue was suspended in 40 mL of toluene, which was subsequently filtered through a short plug of Celite. The collected colored solution was evaporated to dryness, and the resulting semisolid was washed with pentane three times (2 mL each). After drying under a vacuum, the desired product was isolated as a yellow powder (110 mg, 92% yield). ^{1}H NMR (400 MHz, C_6D_6, δ): 8.41 (d, J_{H-H} = 8.4 Hz, Ar*H*, 2H), 7.25 (t, J_{H-H} = 7.4 Hz, Ar*H*, 2H), 7.18 (t, J_{H-H} = 6.8 Hz, Ar*H*, 1H), 6.88 (t, J_{H-H} = 8.0 Hz, Ar*H*, 1H), 6.57 (d, J_{H-H} = 8.0 Hz, Ar*H*, 2H), 2.34−2.24 (m, PC*H*(CH$_3$)$_2$, 4H), 1.38−1.32 (m, PCH(C*H*$_3$)$_2$, 12H), 1.24−1.19 (m, PCH(C*H*$_3$)$_2$,

DOI: 10.1021/acs.organomet.8b00888
Organometallics 2019, 38, 1468−1478

12H). $^{13}C\{^1H\}$ NMR (101 MHz, C_6D_6, δ): 171.04 (s, NiOCOPh), 170.02 (t, J_{P-C} = 10.2 Hz, ArC_{ortho}), 136.56 (s, ArC), 130.54 (s, ArC), 130.21 (s, ArC), 129.26 (s, ArC), 122.48 (t, J_{P-C} = 22.7 Hz, ArC_{ipso}), 105.56 (t, J_{P-C} = 5.8 Hz, ArC_{meta}), 28.93 (t, J_{P-C} = 11.0 Hz, $PCH(CH_3)_2$), 17.79 (t, J_{P-C} = 3.3 Hz, $PCH(CH_3)_2$), 16.96 (s, $PCH(CH_3)_2$). $^{31}P\{^1H\}$ NMR (162 MHz, C_6D_6, δ): 183.55 (s). ATR-IR (solid): ν_{OCO} = 1611 (ν_{asym}), 1569 (ν_{asym}), and 1356 (ν_{sym}) cm^{-1}. Anal. Calcd for $C_{25}H_{36}O_4P_2Ni$: C, 57.61; H, 6.96. Found: C, 57.82; H, 6.81.

Synthesis of NaOPh. Under an argon atmosphere, NaH (480 mg, 20 mmol) was added slowly to a solution of phenol (941 mg, 10 mmol) in 10 mL of THF. The resulting suspension was stirred at room temperature for 30 min and then filtered via a cannula. The collected filtrate was concentrated under a vacuum to yield a white solid (1.10 g, 95% yield), which was used directly for the subsequent synthesis.

Synthesis of {2,6-(^{i}Pr$_2$PO)$_2$C$_6$H$_3$}NiOPh (15). Under an argon atmosphere, **11** (174 mg, 0.40 mmol) and sodium phenoxide (56 mg, 0.48 mmol) were mixed in 10 mL of THF and stirred at room temperature for 16 h. The volatiles were removed under a vacuum, and the residue was suspended in 40 mL of toluene, which was subsequently filtered through a short plug of Celite. The collected colored solution was evaporated to dryness to yield the desired product as a yellow powder (180 mg, 91% yield). ^1H NMR (400 MHz, C_6D_6, δ): 7.28 (t, J_{H-H} = 7.6 Hz, Ar*H*, 2H), 7.11 (d, J_{H-H} = 7.6 Hz, Ar*H*, 2H), 6.85 (t, J_{H-H} = 7.6 Hz, Ar*H*, 1H), 6.71 (t, J_{H-H} = 7.6 Hz, Ar*H*, 1H), 6.54 (d, J_{H-H} = 7.6 Hz, Ar*H*, 2H), 2.02−1.93 (m, $PCH(CH_3)_2$, 4H), 1.28−1.22 (m, $PCH(CH_3)_2$, 12H), 1.20−1.15 (m, $PCH(CH_3)_2$, 12H). $^{13}C\{^1H\}$ NMR (101 MHz, C_6D_6, δ): 170.35 (s, ArC), 169.85 (t, J_{P-C} = 10.2 Hz, ArC_{ortho}), 129.17 (s, ArC), 122.85 (t, J_{P-C} = 22.4 Hz, ArC_{ipso}), 120.61 (s, ArC), 113.82 (s, ArC), 105.65 (t, J_{P-C} = 5.8 Hz, ArC_{meta}), 28.32 (t, J_{P-C} = 10.2 Hz, $PCH(CH_3)_2$), 16.82 (t, J_{P-C} = 3.2 Hz, $PCH(CH_3)_2$), 16.74 (s, $PCH(CH_3)_2$). $^{31}P\{^1H\}$ NMR (162 MHz, C_6D_6, δ): 178.85 (s). Anal. Calcd for $C_{24}H_{36}O_3P_2Ni$: C, 58.45; H, 7.36. Found: C, 58.71; H, 7.65.

X-ray Structure Determination. Crystal data collection and refinement parameters are provided in the Supporting Information. Single crystals of 2,6-(^{i}Pr$_2$PO)$_2$C$_6$H$_3$}NiOC(O)Ph (**14**), {2,6-(^{i}Pr$_2$PO)$_2$C$_6$H$_3$}NiOPh·HOPh (**15**·HOPh), and {2,6-(^{i}Pr$_2$PO)$_2$C$_6$H$_3$}NiOPh (**15**) were grown from pentane, benzene, and THF-pentane, respectively. Intensity data for **14** and **15** were collected at 150 K on a Bruker dual microfocus source D8 Venture Photon-II diffractometer with Mo Kα radiation, λ = 0.71073 Å. Intensity data for **15**·HOPh were collected at 150 K on a Bruker PHOTON-II detector at Beamline 11.3.1 at the Advanced Light Source (Lawrence Berkeley National Laboratory) using synchrotron radiation tuned to λ = 0.7749 Å. The data frames were processed using the program SAINT. The data were corrected for decay, Lorentz, and polarization effects as well as absorption and beam corrections based on the multiscan technique. The structures were solved by a combination of direct methods in SHELXTL and the difference Fourier technique and refined by full-matrix least-squares on F^2. Compound **15** was refined as a twin, 180° rotation about the *a* axis (~6), twin law applied: 1 0 0 0−1 0−0.376 0−1 (Cell_Now). Non-hydrogen atoms were refined with anisotropic displacement parameters. The phenol OH hydrogen in **15**·HOPh was located directly from the difference map, and the coordinates were refined. Remaining hydrogen atoms were calculated and treated with a riding model. The crystal structures for **14**, **15**·HOPh, and **15** have been deposited at the Cambridge Crystallographic Data Centre (CCDC) and allocated the deposition numbers CCDC 1881636−1881638.

■ ASSOCIATED CONTENT

Supporting Information

The Supporting Information is available free of charge on the ACS Publications website at DOI: 10.1021/acs.organomet.8b00888.

NMR and IR spectra of the new nickel pincer complexes, NMR spectra of the reaction between {2,6-(^{i}Pr$_2$PO)$_2$C$_6$H$_3$}NiD (**1-d_1**) and PhCHO, NMR spectra of the catalytic reaction, and X-ray crystallographic information for {2,6-(^{i}Pr$_2$PO)$_2$C$_6$H$_3$}NiOC(O)Ph (**14**), {2,6-(^{i}Pr$_2$PO)$_2$C$_6$H$_3$}NiOPh·HOPh (**15**·HOPh), and {2,6-(^{i}Pr$_2$PO)$_2$C$_6$H$_3$}NiOPh (**15**) (PDF)

Optimized Cartesian coordinates for **14**, **15**·HOPh, and **15** (MOL)

Accession Codes

CCDC 1881636−1881638 contain the supplementary crystallographic data for this paper. These data can be obtained free of charge via www.ccdc.cam.ac.uk/data_request/cif, or by emailing data_request@ccdc.cam.ac.uk, or by contacting The Cambridge Crystallographic Data Centre, 12 Union Road, Cambridge CB2 1EZ, UK; fax: +44 1223 336033.

■ AUTHOR INFORMATION

Corresponding Author

*E-mail: hairong.guan@uc.edu.

ORCID

Hairong Guan: 0000-0002-4858-3159

Notes

The authors declare no competing financial interest.

■ ACKNOWLEDGMENTS

We thank the National Science Foundation (CHE-1464734 and CHE-1800151) for support of this research. Crystallographic data were collected on a Bruker D8 Venture diffractometer (funded by NSF-MRI grant CHE-1625737) or through the SCrALS (Service Crystallography at Advanced Light Source) Program at Beamline 11.3.1 at the Advanced Light Source (ALS), Lawrence Berkeley National Laboratory (funded by the U.S. Department of Energy, Office of Basic Energy Sciences, under contract No. DE-AC02-05CH11231). ^2H NMR experiments were performed on a Bruker AVANCE NEO 400 MHz NMR spectrometer (funded by NSF-MRI grant CHE-1726092).

■ REFERENCES

(1) Seki, T.; Nakajo, T.; Onaka, M. The Tishchenko Reaction: A Classic and Practical Tool for Ester Synthesis. *Chem. Lett.* **2006**, *35*, 824−829.

(2) For representative systems based on Ru, Os, or Ir, see: (a) Murahashi, S.; Ito, K.; Naota, T.; Maeda, Y. Ruthenium Catalyzed Transformation of Alcohols to Esters and Lactones. *Tetrahedron Lett.* **1981**, *22*, 5327−5330. (b) Blum, Y.; Shvo, Y. Catalytically Reactive (η^4-tetracyclone)$(CO)_2(H)_2$Ru and Related Complexes in Dehydrogenation of Alcohols to Esters. *J. Organomet. Chem.* **1985**, *282*, C7−C10. (c) Zhang, J.; Leitus, G.; Ben-David, Y.; Milstein, D. Facile Conversion of Alcohols into Esters and Dihydrogen Catalyzed by New Ruthenium Complexes. *J. Am. Chem. Soc.* **2005**, *127*, 10840−10841. (d) Musa, S.; Shaposhnikov, I.; Cohen, S.; Gelman, D. Ligand-Metal Cooperation in PCP Pincer Complexes: Rational Design and Catalytic Activity in Acceptorless Dehydrogenation of Alcohols. *Angew. Chem., Int. Ed.* **2011**, *50*, 3533−3537. (e) Spasyuk, D.; Smith, S.; Gusev, D. G. From Esters to Alcohols and Back with Ruthenium and Osmium Catalysts. *Angew. Chem., Int. Ed.* **2012**, *51*, 2772−2775. (f) Nielsen, M.; Junge, H.; Kammer, A.; Beller, M. Towards a Green Process for Bulk-Scale Synthesis of Ethyl Acetate: Efficient Acceptorless Dehydrogenation of Ethanol. *Angew. Chem., Int. Ed.* **2012**, *51*, 5711−5713. (g) He, L.-P.; Chen, T.; Gong, D.; Lai, Z.; Huang, K.-W. Enhanced Reactivities Toward Amines by Introducing an Imine Arm to the Pincer Ligand: Direct Coupling of Two Amines to Form an Imine Without Oxidant. *Organometallics* **2012**, *31*, 5208−5211. (h) Zeng, G.; Chen, T.; He, L.; Pinnau, I.; Lai, Z.; Huang, K.-W. A

DOI: 10.1021/acs.organomet.8b00888
Organometallics 2019, 38, 1468−1478

Green Approach to Ethyl Acetate: Quantitative Conversion of Ethanol through Direct Dehydrogenation in a Pd-Ag Membrane Reactor. *Chem. - Eur. J.* **2012**, *18*, 15940−15943. (i) Spasyuk, D.; Vicent, C.; Gusev, D. G. Chemoselective Hydrogenation of Carbonyl Compounds and Acceptorless Dehydrogenative Coupling of Alcohols. *J. Am. Chem. Soc.* **2015**, *137*, 3743−3746. (j) de Boer, S. Y.; Korstanje, T. J.; La Rooij, S. R.; Kox, R.; Reek, J. N. H.; van der Vlugt, J. I. Ruthenium PNN(O) Complexes: Cooperative Reactivity and Application as Catalysts for Acceptorless Dehydrogenative Coupling Reactions. *Organometallics* **2017**, *36*, 1541−1549. (k) Sahoo, A. R.; Jiang, F.; Bruneau, C.; Sharma, G. V. M.; Suresh, S.; Roisnel, T.; Dorcet, V.; Achard, M. Phosphine-Pyridonate Ligands Containing Octahedral Ruthenium Complexes: Access to Esters and Formic Acid. *Catal. Sci. Technol.* **2017**, *7*, 3492−3498. (l) Alabau, R. G.; Esteruelas, M. A.; Martínez, A.; Oliván, M.; Oñate, E. Base-Free and Acceptorless Dehydrogenation of Alcohols Catalyzed by an Iridium Complex Stabilized by a *N,N,N*-Osmaligand. *Organometallics* **2018**, *37*, 2732−2740.

(3) For catalytic systems based on Fe, Co, or Mn, see: (a) Chakraborty, S.; Lagaditis, P. O.; Förster, M.; Bielinski, E. A.; Hazari, N.; Holthausen, M. C.; Jones, W. D.; Schneider, S. Well-Defined Iron Catalysts for the Acceptorless Reversible Dehydrogenation-Hydrogenation of Alcohols and Ketones. *ACS Catal.* **2014**, *4*, 3994−4003. (b) Nguyen, D. H.; Trivelli, X.; Capet, F.; Paul, J.-F.; Dumeignil, F.; Gauvin, R. M. Manganese Pincer Complexes for the Base-Free, Acceptorless Dehydrogenative Coupling of Alcohols to Esters: Development, Scope, and Understanding. *ACS Catal.* **2017**, *7*, 2022−2032. (c) Paudel, K.; Pandey, B.; Xu, S.; Taylor, D. K.; Tyer, D. L.; Torres, C. L.; Gallagher, S.; Kong, L.; Ding, K. Cobalt-Catalyzed Acceptorless Dehydrogenative Coupling of Primary Alcohols to Esters. *Org. Lett.* **2018**, *20*, 4478−4481.

(4) (a) Suzuki, T.; Matsuo, T.; Watanabe, K.; Katoh, T. Iridium-Catalyzed Oxidative Dimerization of Primary Alcohols to Esters Using 2-Butanone as an Oxidant. *Synlett* **2005**, 1453−1455. (b) Bertoli, M.; Choualeb, A.; Lough, A. J.; Moore, B.; Spasyuk, D.; Gusev, D. G. Osmium and Ruthenium Catalysts for Dehydrogenation of Alcohols. *Organometallics* **2011**, *30*, 3479−3482.

(5) Liu, C.; Tang, S.; Lei, A. Oxidant Controlled Pd-Catalysed Selective Oxidation of Primary Alcohol. *Chem. Commun.* **2013**, *49*, 1324−1326.

(6) Hoshimoto, Y.; Ohashi, M.; Ogoshi, S. Nickel-Catalyzed Selective Conversion of Two Different Aldehydes to Cross-Coupled Esters. *J. Am. Chem. Soc.* **2011**, *133*, 4668−4671.

(7) (a) Gowrisankar, S.; Neumann, H.; Beller, M. General and Selective Palladium-Catalyzed Oxidative Esterification of Alcohols. *Angew. Chem., Int. Ed.* **2011**, *50*, 5139−5143. (b) Liu, C.; Wang, J.; Meng, L.; Deng, Y.; Li, Y.; Lei, A. Palladium-Catalyzed Aerobic Oxidative Direct Esterification of Alcohols. *Angew. Chem., Int. Ed.* **2011**, *50*, 5144−5148. (c) Srimani, D.; Balaraman, E.; Gnanaprakasam, B.; Ben-David, Y.; Milstein, D. Ruthenium Pincer-Catalyzed Cross-Dehydrogenative Coupling of Primary Alcohols with Secondary Alcohols under Neutral Conditions. *Adv. Synth. Catal.* **2012**, *354*, 2403−2406.

(8) Curran, S. P.; Connon, S. J. Selenide Ions as Catalysts for Homo- and Crossed-Tishchenko Reactions of Expanded Scope. *Org. Lett.* **2012**, *14*, 1074−1077.

(9) (a) Ekoue-Kovi, K.; Wolf, C. One-Pot Oxidative Esterification and Amidation of Aldehydes. *Chem. - Eur. J.* **2008**, *14*, 6302−6315. (b) Tang, S.; Yuan, J.; Liu, C.; Lei, A. Direct Oxidative Esterification of Alcohols. *Dalton Trans.* **2014**, *43*, 13460−13470.

(10) (a) Murahashi, S.; Naota, T.; Ito, K.; Maeda, Y.; Taki, H. Ruthenium-Catalyzed Oxidative Transformation of Alcohols and Aldehydes to Esters and Lactones. *J. Org. Chem.* **1987**, *52*, 4319−4327. (b) Cheng, J.; Zhu, M.; Wang, C.; Li, J.; Jiang, X.; Wei, Y.; Tang, W.; Xue, D.; Xiao, J. Chemoselective Dehydrogenative Esterification of Aldehydes and Alcohols with a Dimeric Rhodium(II) Catalyst. *Chem. Sci.* **2016**, *7*, 4428−4434.

(11) (a) Grigg, R.; Mitchell, T. R. B.; Sutthivaiyakit, S. Oxidation of Alcohols by Transition Metal Complexes − IV: The Rhodium Catalysed Synthesis of Esters from Aldehydes and Alcohols. *Tetrahedron* **1981**, *37*, 4313−4319. (b) Whittaker, A. M.; Dong, V. M. Nickel-Catalyzed Dehydrogenative Cross-Coupling: Direct Transformation of Aldehydes into Esters and Amides. *Angew. Chem., Int. Ed.* **2015**, *54*, 1312−1315. (c) Liu, H.; Eisen, M. S. Selective Actinide-Catalyzed Tandem Proton-Transfer Esterification of Aldehydes with Alcohols for the Production of Asymmetric Esters. *Organometallics* **2017**, *36*, 1461−1464.

(12) (a) Gopinath, R.; Patel, B. K. A Catalytic Oxidative Esterification of Aldehydes Using V_2O_5-H_2O_2. *Org. Lett.* **2000**, *2*, 577−579. (b) Maki, B. E.; Scheidt, K. A. *N*-Heterocyclic Carbene-Catalyzed Oxidation of Unactivated Aldehydes to Esters. *Org. Lett.* **2008**, *10*, 4331−4334. (c) De Sarkar, S.; Grimme, S.; Studer, A. NHC Catalyzed Oxidations of Aldehydes to Esters: Chemoselective Acylation of Alcohols in Presence of Amines. *J. Am. Chem. Soc.* **2010**, *132*, 1190−1191. (d) Liu, C.; Tang, S.; Zheng, L.; Liu, D.; Zhang, H.; Lei, A. Covalently Bound Benzyl Ligand Promotes Selective Palladium-Catalyzed Oxidative Esterification of Aldehydes with Alcohols. *Angew. Chem., Int. Ed.* **2012**, *51*, 5662−5666.

(13) Finney, E. E.; Ogawa, K. A.; Boydston, A. J. Organocatalyzed Anodic Oxidation of Aldehydes. *J. Am. Chem. Soc.* **2012**, *134*, 12374−12377.

(14) Chakraborty, S.; Krause, J. A.; Guan, H. Hydrosilylation of Aldehydes and Ketones Catalyzed by Nickel PCP-Pincer Hydride Complexes. *Organometallics* **2009**, *28*, 582−586.

(15) (a) Chakraborty, S.; Zhang, J.; Krause, J. A.; Guan, H. An Efficient Nickel Catalyst for the Reduction of Carbon Dioxide with a Borane. *J. Am. Chem. Soc.* **2010**, *132*, 8872−8873. (b) Chakraborty, S.; Patel, Y. J.; Krause, J. A.; Guan, H. Catalytic Properties of Nickel Bis(phosphinite) Pincer Complexes in the Reduction of CO_2 to Methanol Derivatives. *Polyhedron* **2012**, *32*, 30−34. (c) Chakraborty, S.; Zhang, J.; Patel, Y. J.; Krause, J. A.; Guan, H. Pincer-Ligated Nickel Hydridoborate Complexes: the Dormant Species in Catalytic Reduction of Carbon Dioxide with Boranes. *Inorg. Chem.* **2013**, *52*, 37−47.

(16) Chakraborty, S.; Patel, Y. J.; Krause, J. A.; Guan, H. A Robust Nickel Catalyst for Cyanomethylation of Aldehydes: Activation of Acetonitrile under Base-Free Conditions. *Angew. Chem., Int. Ed.* **2013**, *52*, 7523−7526.

(17) (a) Jin, L.-K.; Wan, L.; Feng, J.; Cai, C. Nickel-Catalyzed Regioselective Cross-Dehydrogenative Coupling of Inactive $C(sp^3)$−H Bonds with Indole Derivatives. *Org. Lett.* **2015**, *17*, 4726−4729. (b) Soni, V.; Khake, S. M.; Punji, B. Nickel-Catalyzed $C(sp^2)$−H/$C(sp^3)$−H Oxidative Coupling of Indoles with Toluene Derivatives. *ACS Catal.* **2017**, *7*, 4202−4208. (c) Li, Z.-L.; Sun, K.-K.; Cai, C. Nickel-Catalyzed Cross-Dehydrogenative Coupling of α-$C(sp^3)$−H Bonds in *N*-Methylamides with $C(sp^3)$−H Bonds in Cyclic Alkanes. *Org. Lett.* **2018**, *20*, 6420−6424.

(18) When in equilibrium, deuterium prefers the strongest bond, which in this case would be the acyl−hydrogen (C_{sp2}−H) bond of the aldehyde rather than the benzylic carbon−hydrogen (C_{sp3}−H) bond of the nickel alkoxide complex.

(19) Among complexes {2,6-(^{i}Pr$_2$PO)$_2$C$_6$H$_3$}NiSC$_6$H$_4$X (X = 4-OCH_3, 4-CH_3, H, 4-Cl, and 4-CF_3), the one with the CF_3 substituent has the highest Ni−S bond dissociation energy. For details, see: Zhang, J.; Adhikary, A.; King, K. M.; Krause, J. A.; Guan, H. Substituent Effects on Ni−S Bond Dissociation Energies and Kinetic Stability of Nickel Arylthiolate Complexes Supported by a Bis(phosphinite)-based Pincer Ligand. *Dalton Trans.* **2012**, *41*, 7959−7968.

(20) Related pincer nickel hydroxide complexes also proved to be too unstable for isolation. For examples, see: (a) Hao, J.; Mougang-Soumé, B.; Vabre, B.; Zargarian, D. On the Stability of a $POC_{sp3}OP$-Type Pincer Ligand in Nickel(II) Complexes. *Angew. Chem., Int. Ed.* **2014**, *53*, 3218−3222. (b) Wellala, N. P. N.; Luebking, J. D.; Krause, J. A.; Guan, H. Roles of Hydrogen Bonding in Proton Transfer to $\kappa^P,\kappa^N,\kappa^P$-N(CH$_2CH_2$P^{i}Pr$_2$)$_2$-Ligated Nickel Pincer Complexes. *ACS Omega* **2018**, *3*, 4986−5001.

DOI: 10.1021/acs.organomet.8b00888
Organometallics 2019, 38, 1468−1478

(21) Several pincer nickel hydroxide complexes have been isolated, although the pincer ligands often lack P−O bonds or contain sterically protected P−O bonds. For details, see: (a) Cámpora, J.; Palma, P.; del Río, D.; Álvarez, E. CO Insertion Reactions into the M−OH Bonds of Monomeric Nickel and Palladium Hydroxides. Reversible Decarbonylation of a Hydroxycarbonyl Palladium Complex. *Organometallics* **2004**, *23*, 1652−1655. (b) Castonguay, A.; Beauchamp, A. L.; Zargarian, D. New Derivatives of PCP-Type Pincer Complexes of Nickel. *Inorg. Chem.* **2009**, *48*, 3177−3184. (c) Adhikari, D.; Mossin, S.; Basuli, F.; Dible, B. R.; Chipara, M.; Fan, H.; Huffman, J. C.; Meyer, K.; Mindiola, D. J. A Dinuclear Ni(I) System Having a Diradical Ni_2N_2 Diamond Core Resting State: Synthetic, Structural, Spectroscopic Elucidation, and Reductive Bond Splitting Reactions. *Inorg. Chem.* **2008**, *47*, 10479−10490. (d) Zargarian, D.; Salah, A. [2,6-Bis(diphenylphosphanyloxy)phenyl-κ^3P,C^1,P']hydroxidonickel-(II). *Acta Crystallogr., Sect. E: Struct. Rep. Online* **2011**, *67*, m940. (e) Jonasson, K. J.; Mousa, A. H.; Wendt, O. F. Synthesis and Characterisation of $POC_{sp3}OP$ Supported Ni(II) Hydroxo, Hydroxycarbonyl and Carbonate Complexes. *Polyhedron* **2018**, *143*, 132−137. (f) Mousa, A. H.; Bendix, J.; Wendt, O. F. Synthesis, Characterization, and Reactivity of PCN Pincer Nickel Complexes. *Organometallics* **2018**, *37*, 2581−2593.

(22) A similar protonation reaction was observed between {2,6-(^{i}Pr$_2$PCH$_2$)$_2$C$_6$H$_3$}NiH and MeOH. For details, see: Martínez-Prieto, L. M.; Ávila, E.; Palma, P.; Álvarez, E.; Cámpora, J. *β*-Hydrogen Elimination Reactions of Nickel and Palladium Methoxides Stabilised by PCP Pincer Ligands. *Chem. - Eur. J.* **2015**, *21*, 9833−9849.

(23) (a) Hao, J.; Vabre, B.; Zargarian, D. POCOP-Ligated Nickel Siloxide Complexes: Syntheses, Characterization, and Reactivities. *Organometallics* **2014**, *33*, 6568−6576. (b) Adhikary, A.; Krause, J. A.; Guan, H. Configurational Stability and Stereochemistry of P-Stereogenic Nickel POCOP-Pincer Complexes. *Organometallics* **2015**, *34*, 3603−3610.

(24) Martínez-Prieto, L. M.; Palma, P.; Álvarez, E.; Cámpora, J. Nickel Pincer Complexes with Frequent Aliphatic Alkoxo Ligands [(^{iPr}PCP)Ni-OR] (R = Et, *n*Bu, *i*Pr, 2-hydroxyethyl). An Assessment of the Hydrolytic Stability of Nickel and Palladium Alkoxides. *Inorg. Chem.* **2017**, *56*, 13086−13099.

(25) Jonasson, K. J.; Wendt, O. F. Synthesis and Characterization of a Family of POCOP Pincer Complexes with Nickel: Reactivity Towards CO_2 and Phenylacetylene. *Chem. - Eur. J.* **2014**, *20*, 11894−11902.

(26) (a) Enthaler, S.; Brück, A.; Kammer, A.; Junge, H.; Irran, E.; Gülak, S. Exploring the Reactivity of Nickel Pincer Complexes in the Decomposition of Formic Acid to CO_2/H_2 and the Hydrogenation of $NaHCO_3$ to HCOONa. *ChemCatChem* **2015**, *7*, 65−69. (b) Ma, Q.-Q.; Liu, T.; Adhikary, A.; Zhang, J.; Krause, J. A.; Guan, H. Using CS_2 to Probe the Mechanistic Details of Decarboxylation of Bis-(phosphinite)-Ligated Nickel Pincer Formate Complexes. *Organometallics* **2016**, *35*, 4077−4082. (c) Osipova, E. S.; Belkova, N. V.; Epstein, L. M.; Filippov, O. A.; Kirkina, V. A.; Titova, E. M.; Rossin, A.; Peruzzini, M.; Shubina, E. S. Dihydrogen Bonding and Proton Transfer from MH and OH Acids to Group 10 Metal Hydrides [(^{tBu}PCP)MH] [^{tBu}PCP = κ^3-2,6-(*t*Bu$_2$PCH$_2$)$_2$C$_6$H$_3$; M = Ni, Pd]. *Eur. J. Inorg. Chem.* **2016**, *2016*, 1415−1424.

(27) Li, H.; Meng, W.; Adhikary, A.; Li, S.; Ma, N.; Zhao, Q.; Yang, Q.; Eberhardt, N. A.; Leahy, K. M.; Krause, J. A.; Zhang, J.; Chen, X.; Guan, H. Metathesis Reactivity of Bis(phosphinite) Pincer Ligated Nickel Chloride, Isothiocyanate and Azide Complexes. *J. Organomet. Chem.* **2016**, *804*, 132−141.

(28) Pandarus, V.; Zargarian, D. New Pincer-Type Diphosphinito (POCOP) Complexes of Nickel. *Organometallics* **2007**, *26*, 4321−4334.

DOI: 10.1021/acs.organomet.8b00888
Organometallics 2019, 38, 1468−1478